DOI 10.1007/s10517-023-05827-w

KDM5 Family Demethylase Inhibitor KDOAM-25 Reduces Entry of SARS-CoV-2 Pseudotyped Viral Particles into Cells

E. N. Knyazev[1,2], R. S. Kalinin[1], V. A. Abrikosova[1], Yu. A. Mokrushina[1], and S. A. Tonevitskaya[2]

Translated from *Kletochnye Tekhnologii v Biologii i Meditsine*, No. 1, pp. 40-46, March, 2023
Original article submitted November 3, 2022

We studied the effect of KDM5 family demethylase inhibitors (JIB-04, PBIT, and KDOAM-25) on the penetration of SARS-CoV-2 pseudotyped viruses into differentiated Caco-2 cells and HEK293T cells with *ACE2* hyperexpression. The above drugs were not cytotoxic. Only KDOAM-25 significantly reduced virus entry into the cells. The expression of *ACE2* mRNA in Caco-2 significantly increased, while *TMPRSS2* expression did not significantly change under these conditions. In differentiated Caco-2 cells, KDOAM-25 did not affect the expression of *BRCA1*, *CDH1*, *TP53*, *SNAI1*, *VIM*, and *UGCG* genes, for which an association with knockdown or overexpression of KDM5 demethylases or with the action of demethylase inhibitors had previously been shown. In undifferentiated Caco-2 cells, the expression of *BRCA1*, *SNAI1*, *VIM*, and *CDH1* was significantly increased under the action of KDOAM-25.

Key Words: *demethylase; KDM5; COVID-19; SARS-CoV-2; coronavirus*

One of the strategies to combat the SARS-CoV-2 that causes COVID-19 is to prevent the virus from binding to the cell membrane and entering the cell, which can be achieved through the production of natural antibodies or the use of artificial antibodies or drugs that affect various steps of the virus life cycle. The search for potential drugs to combat SARS-CoV-2 remains relevant since the emergence of new strains of the virus reduces the effectiveness of vaccines and antibodies [1]. One of the approaches in the search for potential therapy is the selection of molecules directed against angiotensin-converting enzyme 2 (ACE2), which is a receptor for the entry of SARS-CoV-2 into cells, or cellular proteases involved in cutting the spike protein (S protein) of SARS-CoV-2, for example, transmembrane serine protease TMPRSS2 [2]. However, it was found that SARS-CoV-2 can use other molecules for binding to the membrane and entering the cells, such as neuropilin 1 (NRP1), basigin (BSG/CD147), and dipeptidyl peptidase 4 (DPP4) [3,4].

Previously, it was shown that lysine-specific demethylase 5B (KDM5B, JARID1B, or PLU1) can reduce the expression of microRNA families hsa-let-7e/hsa-miR-125a and hsa-miR-141/hsa-miR-200 due to the removal of H3K4me3 methyl tags from histones H3 in the regulatory regions of these microRNAs. Since the targets of these miRNAs are the *ACE2* and *TMPRSS2* genes, it has been suggested that inhibitors of KDM5B demethylase can decrease the expression of these genes and prevent the entry of SARS-CoV-2 into cells [5]. One of the most specific KDM5B inhibitors known so far is KDOAM-25, which has demonstrated low cytotoxicity and high stability and specificity against KDM5 family demethylases with the highest specificity for KDM5B demethylase: a half-maximal inhibition concentration (IC_{50}) of 19 nM against KDM5B demethylase *in vitro* and 50 μM in the cell system. At the same time, the drug did not inhibit other demethy-

[1]M. M. Shemyakin and Yu. A. Ovchinnikov Institute of Bioorganic Chemistry, Russian Academy of Sciences, Moscow, Russia; [2]Faculty of Biology and Biotechnologies, National Research University Higher School of Economics, Moscow, Russia. ***Address for correspondence:*** eknyazev@hse.ru. E. N. Knyazev

lases of the JmjC family [6]. The higher IC_{50} value in the cell system compared to *in vitro* conditions can be explained by partial competition with the cofactor α-ketoglutarate and the relatively low permeability of the cell membrane for the drug, which was confirmed in Caco-2 cells [6]. On the other hand, other known KDM5B demethylase inhibitors, in contrast to KDOAM-25, are characterized by lower specificity. The IC_{50} of the PBIT inhibitor against KDM5B was about 3 μM *in vitro* [7], for aspartate/asparagine-β-hydroxylase it was 0.14 μM *in vitro* [8], and for tryptophan hydroxylase 1 it was 0.096 μM *in vitro* and 0.528 μM in the cell system [9], which raises the question of its specificity against demethylases of the KDM5 family. Another potential inhibitor of KDM5 demethylases is JIB-04, a pan-inhibitor of histone demethylases from the Jumonji family. JIB-04 has IC_{50} ~5 μM *in vitro* against the KDM5B fragment [7], but also inhibited demethylases of the KDM4 and KDM6 families [10].

Biosafety level 3 laboratories are required to study SARS-CoV-2 *in vivo*, so many studies are conducted on pseudotyped viral particles. For the analysis of SARS-CoV-2, packaging systems based on lentiviruses, mouse leukemia virus, vesicular stomatitis virus, and other viruses can be used, which include the S-protein of SARS-CoV-2 and plasmids, which make it possible to detect infection of cells with pseudotyped particles, for example, by activity of the luciferase gene or fluorescent proteins [11]. Various cell systems can be used to study wild-type and pseudotyped viruses, including immortalized cell lines (Caco-2, Vero E6, Huh-7, A549, *etc.*) and primary cells with *ACE2* expression, as well as cell lines with artificial *ACE2* overexpression [12].

This work aimed to study the effect of demethylase inhibitors of the KDM5 family on the penetration of SARS-CoV-2 pseudotyped viral particles into Caco-2 cells and modified HEK293T cells with *ACE2* overexpression. To assess the effect of demethylase inhibitors, we chose two cell lines with fundamentally different regulation of *ACE2* gene activity: Caco-2 in which *ACE2* is regulated by natural cellular mechanisms, and HEK293T transfected with *ACE2* under the control of the cytomegalovirus promoter.

MATERIALS AND METHODS

Pseudotyped SARS-CoV-2 virus particles were derived from the HIV-1 lentivirus. HEK293T cells were transfected with a plasmid carrying the SARS-CoV-2 S protein gene under the control of the CAG promoter, a plasmid carrying the HIV-1 *gag-pol* gene, and a plasmid encoding a recombinant RNA genome containing the firefly luciferase gene.

Caco-2 cells were obtained from the Russian Collection of Cell Cultures (Institute of Cytology, Russian Academy of Sciences, St. Petersburg). Cells were cultured in Gibco MEM medium with 20% Gibco FBS OneShot, 1% Gibco GlutaMAX Supplement, 1% Gibco PenStrep (100 U/ml penicillin and 100 μg/ml streptomycin) (all components Thermo Fisher Scientific). To obtain a monolayer of differentiated Caco-2 cells, culturing was continued after reaching a confluent monolayer for 21 days. Differentiation was monitored by impedance spectroscopy of Caco-2 cells on Transwell culture inserts (Corning) [13].

HEK293T cells were transfected with a genetic construct based on the pCDH-CMV-MCS lentiviral plasmid containing the cDNA sequence of the *ACE2* gene under the control of the cytomegalovirus promoter (HEK293T-ACE2). Cells were cultured in Gibco DMEM high glucose medium (Thermo Fisher Scientific) supplemented with 10% Gibco FBS OneShot, 1% Gibco GlutaMAX Supplement, 1% Gibco PenStrep (100 U/ml penicillin and 100 μg/ml streptomycin) (all components were from Thermo Fisher Scientific).

HEK293T-ACE2 cells and differentiated Caco-2 cells were seeded in 96-well plates; 25 or 50 μM KDOAM-25, 5 or 10 μM PBIT, 2 or 0.6 μM JIB-04, or control medium with 0.1% DMSO were added. After 72 h, the culture medium was changed to a new portion with viral particles and incubated for another 72 h. After that, the cells were lysed according to the Luciferase Cell Culture Lysis 5X Reagent (Promega) protocol and 20 μl of the lysate were transferred into white 96-well plates, 100 μl of the reagent with luciferin and produced a reading of the luminescence. Composition of the luciferin reagent: 100 mM Tris, 60 mM $MgSO_4$, 5 mM DTT, 4 mM EDTA, 4 mM ATP, 0.6 mM luciferin, 0.1 mM $Na_4P_2O_7$, 10% glycerol, and deionized water to final volume.

The cytotoxicity of the preparations was assessed in 96-well plates using the MTT Assay Kit (Abcam) 24 and 72 h after incubation with demethylase inhibitors.

For PCR, HEK293T-ACE2 cells and differentiated and undifferentiated Caco-2 cells were incubated for 72 h in 6-well plates with 50 μM KDOAM-25 or under control conditions with 0.1% DMSO and lysed in 700 μl of QIAzol Lysis Reagent (Qiagen). RNA was isolated from lysates using the miRNeasy Mini Kit according to the manufacturer's protocol with a DNase treatment step on columns and elution in 30 μl of water. The concentration of total RNA was determined using a NanoDrop ND-1000 spectrophotometer; RNA quality was assessed using the RNA StdSens Analysis Kit on an Experion instrument (Bio-Rad) [14].

Reverse transcription was performed from 750 ng of total RNA in a volume of 20 μl using the MMLV RT kit (Eurogen) according to the manufacturer's protocol. PCR was performed in 384-well plates in a volume of 12.5 μl using the qPCRmix-HS SYBR reagent kit

(Eurogen) according to the manufacturer's protocol. *ACTB* was used as a reference gene. Primers for PCR are shown in Table 1.

Cell viability was compared under different conditions using a two-tailed Student's *t* test. Changes were considered significant at $p<0.05$. Visualization and statistical comparison of relative luminescence during infection with pseudotyped viral particles were performed in the R.Studio program based on the R programming language using the ggpubr package and the Wilcoxon's test to assess statistical significance ($p<0.05$). Differences in gene expression were considered significant if the fold change in expression was at least 1.5-fold and $p<0.05$ using a two-tailed Student's *t* test.

TABLE 1. Primer Sequences for PCR

Gene	Sequence
ACTB	F: CTGAACGGTGAAGGTGACA
	R: AAGGGACTTCCTGTAACAACGCA
ACE2	F: AGAGAAGTGGAGGTGGATGGTCTTT
	R: GCGGGGTCACAGTATGTTTCATCA
TMPRSS2	F: AACGAGAACTACGGGCGGGC
	R: CGCTGTCATCCACTATTCCTTGGC
BRCA1	F: GCGGGAGGAAAATGGGTAGTTAG
	R: AACAGATTTCTAGCCCCCTGAAGA
CDH1	F: CGACACCCGATTCAAAGTGG
	R: TCCCAGGCGTAGACCAAGAA
TP53	F: TGTGGTGGTGCCCTATGAGCC
	R: ATGTAGTTGTAGTGGATGGTGGT
SNAI1	F: CTAGCGAGTGGTTCTTCTG
	R: CTGCTGGAAGGTAAACTCTG
VIM	F: GCAGGAGGAGATGCTTCAGAGA
	R: AAGGTCAAGACGTGCCAGAGAC
UGCG	F: GAGCGTTGTCCGTGTTGG
	R: TCAGTTGCCTTCTTGTTGAGG
HNF4A	F: CACGGGCAAACACTACGGT
	R: TTGACCTTCGAGTGCTGATCC
SOX2	F: CGCAGACCTACATGAACG
	R: GGACTTGACCACCGAACC
DDIT4	F: GTTTGACCGCTCCACGAGCC
	R: CGAAGTCGGGCAACGACACC
PROM1	F: CCAGTGCTTCCTGCTCCTCTT
	R: AACTTGGTGCCTCCTGCCT
PTEN	F: CTCAGCCGTTACCTGTGTGTGG
	R: TGAGGTTTCCTCTGGTCCTGGTATG
MALAT1	F: AGCAGTTCGTGGTGAAGATAG
	R: CATATTGCCGACCTCACG
EGR1	F: AACGAGAAGGTGCTGGTGGAGA
	R: AGATGGTGCTGAGGACGAGGAG
CDKN1B	F: AGGAGAGCCAGGATGTCAGC
	R: ACCAAATGCGTGTCCTCAGA
BSG	F: GCAGGTTCTTCGTGAGTTCC
	R: GGCGTCGTCATCATCCA
DPP4	F: TTTCTTTGCAGTGGCTCAGGAGG
	R: GCCTAAATCTTCCAACCCAGCC

RESULTS

Evaluation of the cytotoxicity of demethylase inhibitors KDOAM-25, PBIT and JIB-04 using the MTT test revealed no significant changes in the viability of HEK293T-ACE2 and differentiated Caco-2 cells for 24 and 72 h. Figure 1 shows the relative viability of cells exposed to KDOAM inhibitor, because we later found that only this drug affected the penetration of pseudotyped viral particles into the cells. The results obtained are consistent with data on the low cytotoxicity of KDOAM-25 [7]. The PBIT inhibitor in a concentration of 10 μM induced death of UACC-812 cells with high expression of *KDM5B*, but had almost no effect on MCF7 and MCF10A cells with lower expression of this gene [15]. In the study of colorectal cancer lines, the JIB-04 inhibitor dose-dependently reduced the viability of HCT-116 cells but had almost no effect on the HT-29 and DLD-1 lines [16]. The IC_{50} of PBIT and JIB-04 varied significantly for different cell lines [17]. The impact of demethylase inhibitors on cells can largely depend on the level of demethylase expression and activity of intracellular signaling systems. In our experiment, KDOAM-25, PBIT, and JIB-04 in the studied concentrations were not toxic for HEK293T-ACE2 and differentiated Caco-2 cells.

The effect of demethylase inhibitors KDOAM-25, PBIT, and JIB-04 on the entry of pseudotyped SARS-CoV-2 viral particles into differentiated Caco-2 cells and HEK293T-ACE2 cells was also evaluated. The number of viral particles entering the cells under different conditions was determined by luminescence expressed as a percentage relative to the control conditions. KDOAM-25, a selective demethylase inhibitor of the KDM5 family, led to a decrease in infection of differentiated Caco-2 cells by 2.9 times in a concentration of 25 μM and by 7.6 times in a concentration of 50 μM (Fig. 2, *a*), while infection of HEK293T-ACE2 cells decreased by about 1.7 times in the presence of both concentrations (Fig. 2, *b*). At the same time, the demethylase inhibitor PBIT in concentrations of 5 and 10 μM and the JIB-04 inhibitor in concentrations of 2 and 0.6 μM did not significantly affect cell infection.

One of the hypotheses suggests the presence of regulatory links between demethylases of the KDM5

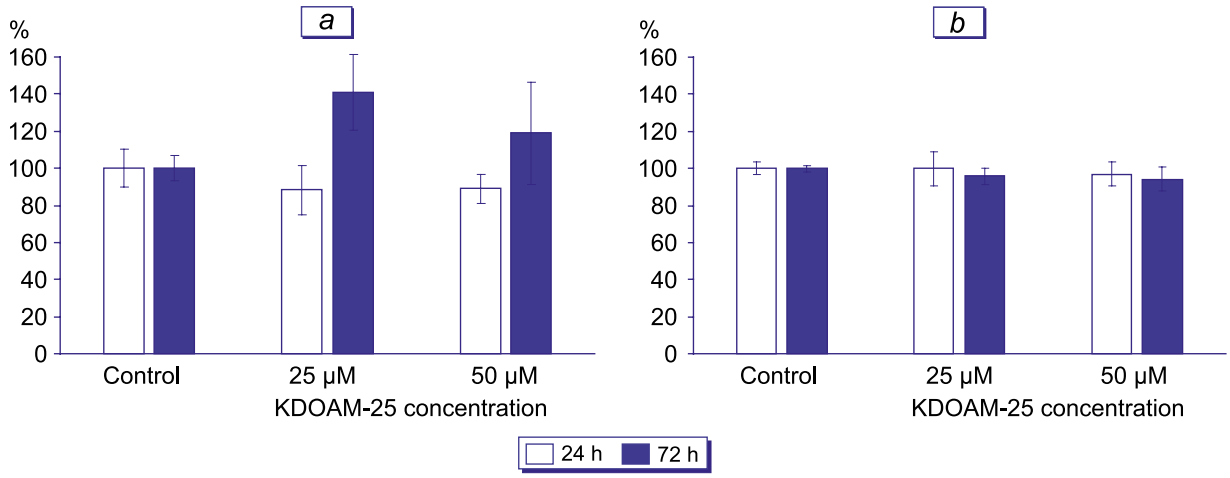

Fig. 1. Relative cytotoxicity of demethylase inhibitor KDOAM-25 in concentrations of 25 and 50 μM against differentiated Caco-2 cells (*a*) and HEK293T-ACE2 cells (*b*) after 24- and 72-h culturing.

family, in particular KDM5B, and the expression of *ACE2* and *TMPRSS2* [18]. The effect of the KDOAM-25 inhibitor on HEK293T-ACE2 cells and differentiated and undifferentiated Caco-2 cells was assessed by changes in the expression of the *ACE2* and *TMPRSS2* genes over 72 h. In HEK293T-ACE2 cells, in which stable *ACE2* expression is maintained due to transfection with a plasmid with the *ACE2* gene under the control of the cytomegalovirus promoter, no significant change in *ACE2* expression was observed, and the expression of the *TMPRSS2* gene was not detected at the level sufficient for analysis of its change. At the same time, in differentiated Caco-2 cells exposed to KDOAM-25, *ACE2* expression increased by 1.7 times (p=0.041), while *TMPRSS2* expression did not change significantly (fold change 0.7, p=0.499). In undifferentiated Caco-2 cells, *ACE2* expression increased by 2.1 times (p=0.015), while *TMPRSS2* expression also did not change significantly (fold change 1.4, p=0.377).

Previously, it was shown that PBIT has a minimal effect on the SARS-CoV-2 nsp14–nsp10 nuclease complex. At the same time, its analogue ebselen, in which the sulfur atom is replaced by selenium, strongly suppresses the activity of this complex [19]. The effect of KDOAM-25 and PBIT on the entry of the SARS-CoV-2 coronavirus into cells has not been studied. However, the JIB-04 inhibitor has been shown to reduce the infection of Vero E6 cells. At the same time, the researchers concluded that this effect was not related to the stage of virus entry into the cell and was caused by violation of the stability or transcription of viral RNA at an early stage after entering the cells. At the same time, the knockdown of *KDM4B*, *KDM4C*, *KDM5A*, and *KDM5B* demethylase genes also mimicked the effects of JIB-04 on cell infection with viruses [20]. In our experiment, we used pseudotyped SARS-CoV-2 viral particles that do not express viral RNA. This can explain why JIB-04 did not affect the

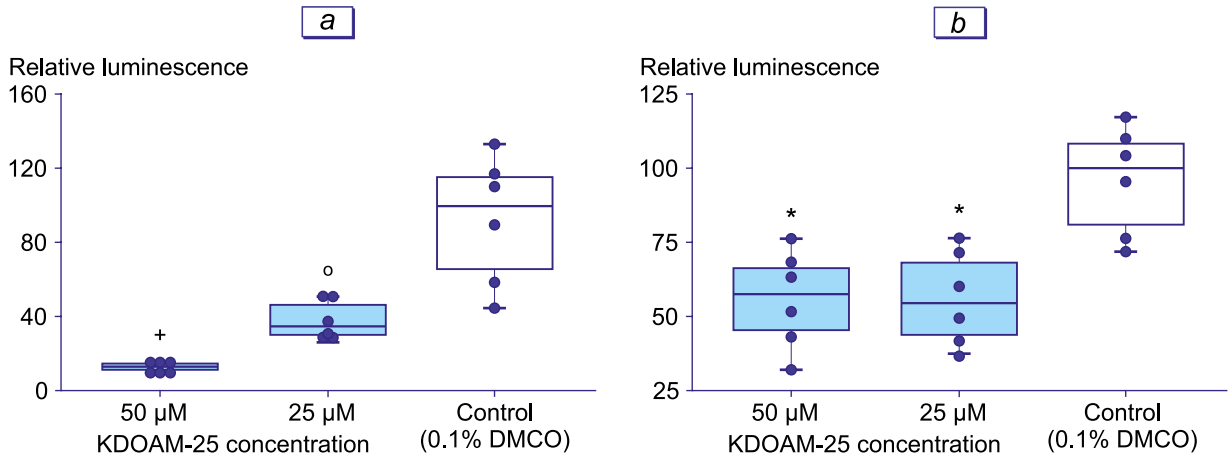

Fig. 2. Relative luminescence upon incubation of differentiated Caco-2 cells (*a*) and HEK293T-ACE2 cells (*b*) with pseudotyped SARS-CoV-2 particles after exposure to KDOAM-25 inhibitor in concentrations of 25 and 50 μM. ^{+}p=0.005, ^{o}p=0.0087, $^{*}p$=0.0043 in comparison with the control.

infection of HEK293T and Caco-2 cells. At the same time, KDOAM-25 significantly reduced the penetration of viral particles into the cell, but *ACE2* expression did not decrease and increased instead. Since the increase in the expression at the mRNA level does not mean similar changes at the protein level, the regulation of *ACE2* through KDM5 demethylases cannot be ruled out. However, there may be other, as yet unexplained, reasons behind the observed effect. The study of the promoter region of the *ACE2* gene revealed a large number of H3K4me3 methyl marks in the kidneys, heart, and small intestine and a small amount in the lungs and HUVEC endothelial cells, which correlates with the level of *ACE2* expression in these tissues [21]. KDOAM-25, as an inhibitor of KDM5B demethylase, can directly increase the activity of the *ACE2* gene in Caco-2 cells, similar to cells of the small intestine epithelium. Still, this effect was not observed in HEK293T cells derived from the kidney since the cells already express *ACE2* on an elevated level due to the cytomegalovirus promoter, which is not subject to natural regulation by cellular systems. At the same time, the decrease in the penetration of viral particles into cells was explained not by the regulation of the *ACE2* and *TMPRSS2* genes but by other mechanisms.

SARS-CoV-2 can use basigin (BSG/CD147) and DPP4 to attach to the membrane and enter astrocytes [3]. According to our earlier sequencing of Caco-2 cells [22], the expression level of the *BSG* and *DPP4* genes is several orders of magnitude higher than the expression level of *ACE2*. However, we did not find statistically significant changes in the expression of these genes under the influence of KDOAM-25. Other mechanisms are involved in decreasing the penetration of viral particles into cells under the action of KDOAM-25, in addition to regulating receptors on the cell surface. Thus, it was shown that KDM5B demethylase could regulate the expression of the *CAV1* gene encoding the caveolin protein involved in one of the types of endocytosis [23], which can also be a potential mechanism for regulating the entry of SARS-CoV-2 into cells.

We have searched for genes whose expression can potentially change under the influence of KDOAM-25. In the available literature, there are no data on the effect of KDOAM-25 on the expression of various genes in cells. According to preliminary data, KDOAM-25 added to modified breast cancer MCF-7 cells increases the expression of the *UGCG* gene by ~2 times in a concentration of 30 μM and by about 1.5 times in a concentration of 50 μM [24]. We also performed a search for genes whose expression changes upon knockdown or overexpression of the demethylase genes of the KDM5 family or upon exposure to PBIT and JIB-04 inhibitors to assess the changes in these genes under the influence of KDOAM-25. Knockdown of the *KDM5B* gene led to changes in the expression of the *BRCA1*, *PTEN*, and *TP53* genes in MCF7 cells [23]. Knockdown of the *KDM5B* gene in MCF10A cells was associated with a decrease in the expression level of SNAI1 and VIM at the protein level, according to Western blot data. Overexpression of *KDM5B* led to an increase in the expression of *SNAI1* and *VIM* according to PCR data, which, according to the researchers, occurred indirectly through the regulation of *MALAT1* gene expression [25]. *KDM5B* overexpression reduced the *EGR1* and *CDKN1B* gene expression in mouse stem cells [26]. The JIB-04 inhibitor led to increased expression of the *CDH1* and *PROM1* genes in colorectal cancer cells and fibroblasts [16], *SOX2* in fibroblasts [27], *DDIT4* in the Tcam-2, 2102EP, and JAR lines [17], while PBIT changed the expression of *VIM*, *CDH1*, and *SOX2* in non-small cell lung cancer cells [28] and expression of the *HNF4A* gene in mouse hepatocytes [29].

In our experiment, in differentiated Caco-2 cells after exposure to KDOAM-25, no significant changes in the expression of the *BRCA1*, *CDH1*, *TP53*, *SNAI1*, *VIM*, and *UGCG* genes were detected. Differentiated Caco-2 cells are more resistant to various influences, probably due to deep morphofunctional differentiation and the absence of active division [30]. Therefore, we also evaluated the effect of KDOAM-25 on gene expression in undifferentiated Caco-2 cells. There was a significant increase in the expression of *BRCA1* (by 2.7 times, p=0.049), *SNAI1* (by 2.3 times, p=0.039), *VIM* (by 1.7 times, p=0.014), and *CDH1* (by 1.7 times, p=0.020) gene expression. In undifferentiated Caco-2, there was no significant change in the expression of the *TP53*, *UGCG*, *HNF4A*, *SOX2*, *DDIT4*, *PROM1*, *PTEN*, *MALAT1*, *EGR1*, and *CDKN1B* genes, for which an association with the expression of demethylases of the KDM5 family and the action of their inhibitors was found.

Thus, the studied demethylase inhibitors of the KDM5 family JIB-04, PBIT, and KDOAM-25 had no cytotoxic effect on differentiated Caco-2 cells and HEK293T cells with increased *ACE2* expression. At the same time, only KDOAM-25 significantly reduced the entry of SARS-CoV-2 pseudotyped viral particles into cells. KDOAM-25 significantly increased *ACE2* expression at the mRNA level in differentiated and undifferentiated Caco-2, which may indicate the absence of a relationship between *ACE2* expression at the mRNA and protein levels or the presence of another mechanism for regulating the cell entry of SARS-CoV-2 under the action of KDOAM-25. In differentiated Caco-2, there was no significant change in the expression of genes associated with knockdown or overexpression of the *KDM5B* gene or the action of other demethylase

inhibitors. However, in undifferentiated Caco-2, there was a significant increase in the expression of the *BRCA1*, *SNAI1*, *VIM*, and *CDH1* genes. The mechanism of influence of KDOAM-25 on the penetration of SARS-CoV-2 into cells requires further study.

The work was supported by a grant from the Ministry of Education and Science of the Russian Federation (Agreement No. 075-15-2021-1049).

REFERENCES

1. Laurie MT, Liu J, Sunshine S, Peng J, Black D, Mitchell AM, Mann SA, Pilarowski G, Zorn KC, Rubio L, Bravo S, Marquez C, Sabatino JJ, Mittl K, Petersen M, Havlir D, DeRisi J. SARS-CoV-2 variant exposures elicit antibody responses with differential cross-neutralization of established and emerging strains including Delta and Omicron. J. Infect. Dis. 2022;225(11):1909-1914. doi: 10.1093/infdis/jiab635
2. Ashour NA, Abo Elmaaty A, Sarhan AA, Elkaeed EB, Moussa AM, Erfan IA, Al-Karmalawy AA. A systematic review of the global intervention for SARS-CoV-2 combating: from drugs repurposing to Molnupiravir approval. Drug Des. Devel. Ther. 2022;16:685-715. doi: 10.2147/DDDT.S354841
3. Huang S, Fishell G. In SARS-CoV-2, astrocytes are in it for the long haul. Proc. Natl Acad. Sci. USA. 2022;119(30):e2209130119. doi: 10.1073/pnas.2209130119
4. Knyazev E, Nersisyan S, Tonevitsky A. Endocytosis and transcytosis of SARS-CoV-2 across the intestinal epithelium and other tissue barriers. Front. Immunol. 2021;12:636966. doi: 10.3389/fimmu.2021.636966
5. Nersisyan S, Shkurnikov M, Turchinovich A, Knyazev E, Tonevitsky A. Integrative analysis of miRNA and mRNA sequencing data reveals potential regulatory mechanisms of ACE2 and TMPRSS2. PLoS One. 2020;15(7):e0235987. doi: 10.1371/journal.pone.0235987
6. Tumber A, Nuzzi A, Hookway ES, Hatch SB, Velupillai S, Johansson C, Kawamura A, Savitsky P, Yapp C, Szykowska A, Wu N, Bountra C, Strain-Damerell C, Burgess-Brown NA, Ruda GF, Fedorov O, Munro S, England KS, Nowak RP, Schofield CJ, La Thangue NB, Pawlyn C, Davies F, Morgan G, Athanasou N, Müller S, Oppermann U, Brennan PE. Potent and selective KDM5 inhibitor stops cellular demethylation of H3K4me3 at transcription start sites and proliferation of MM1S myeloma cells. Cell Chem. Biol. 2017;24(3):371-380. doi: 10.1016/j.chembiol.2017.02.006
7. Zheng YC, Chang J, Wang LC, Ren HM, Pang JR, Liu HM. Lysine demethylase 5B (KDM5B): A potential anti-cancer drug target. Eur. J. Med. Chem. 2019;161:131-140. doi: 10.1016/j.ejmech.2018.10.040
8. Brewitz L, Tumber A, Pfeffer I, McDonough M.A, Schofield CJ. Aspartate/asparagine-β-hydroxylase: a high-throughput mass spectrometric assay for discovery of small molecule inhibitors. Sci. Rep. 2020;10(1):8650. doi: 10.1038/s41598-020-65123-9
9. Betari N, Sahlholm K, Ishizuka Y, Teigen K, Haavik J. Discovery and biological characterization of a novel scaffold for potent inhibitors of peripheral serotonin synthesis. Future Med. Chem. 2020;12(16):1461-1474. doi: 10.4155/fmc-2020-0127
10. Wang L, Chang J, Varghese D, Dellinger M, Kumar S, Best AM, Ruiz J, Bruick R, Peña-Llopis S, Xu J, Babinski DJ, Frantz DE, Brekken RA, Quinn AM, Simeonov A, Easmon J, Martinez ED. A small molecule modulates Jumonji histone demethylase activity and selectively inhibits cancer growth. Nat. Commun. 2013;4:2035. doi: 10.1038/ncomms3035
11. Chen M, Zhang XE. Construction and applications of SARS-CoV-2 pseudoviruses: a mini review. Int. J. Biol. Sci. 2021;17(6):1574-1580. doi: 10.7150/ijbs.59184
12. Rosa RB, Dantas WM, do Nascimento JCF, da Silva MV, de Oliveira RN, Pena LJ. In vitro and in vivo models for studying SARS-CoV-2, the etiological agent responsible for COVID-19 pandemic. Viruses. 2021;13(3):379. doi: 10.3390/v13030379.
13. Nikulin SV, Knyazev EN, Gerasimenko TN, Shilin SA, Gazizov IN, Zakharova GS, Poloznikov AA, Sakharov DA. Impedance spectroscopy and transcriptome analysis of choriocarcinoma BeWo b30 as a model of human placenta. Mol. Biol. (Mosk). 2019;53(3):467-475. doi: 10.1134/S0026898419030133
14. Knyazev EN, Nyushko KM, Alekseev BY, Samatov TR, Shkurnikov MY. Suppression of ITGB4 gene expression in PC-3 cells with short interfering RNA induces changes in the expression of β-integrins associated with RGD-receptors. Bull. Exp. Biol. Med. 2015;159(4):541-545. doi: 10.1007/s10517-015-3011-9
15. Sayegh J, Cao J, Zou MR, Morales A, Blair LP, Norcia M, Hoyer D, Tackett AJ, Merkel JS, Yan Q. Identification of small molecule inhibitors of Jumonji AT-rich interactive domain 1B (JARID1B) histone demethylase by a sensitive high throughput screen. J. Biol. Chem. 2013;288(13):9408-9417. doi: 10.1074/jbc.M112.419861
16. Kim MS, Cho HI, Yoon HJ, Ahn YH, Park EJ, Jin YH, Jang YK. JIB-04, a small molecule histone demethylase inhibitor, selectively targets colorectal cancer stem cells by inhibiting the Wnt/β-catenin signaling pathway. Sci. Rep. 2018;8(1):6611. doi: 10.1038/s41598-018-24903-0
17. Müller MR, Burmeister A, Skowron MA, Stephan A, Bremmer F, Wakileh GA, Petzsch P, Köhrer K, Albers P, Nettersheim D. Therapeutical interference with the epigenetic landscape of germ cell tumors: a comparative drug study and new mechanistical insights. Clin. Epigenetics. 2022;14(1):5. doi: 10.1186/s13148-021-01223-1
18. Nersisyan SA, Shkurnikov MY, Osipyants AI, Vechorko VI. Role of ACE2/TMPRSS2 genes regulation by intestinal microRNA isoforms in the COVID-19 pathogenesis. Bulletin of RSMU. 2020;(2):16-18. doi: 10.24075/brsmu.2020.024
19. Baddock HT, Brolih S, Yosaatmadja Y, Ratnaweera M, Bielinski M, Swift LP, Cruz-Migoni A, Fan H, Keown JR, Walker AP, Morris GM, Grimes JM, Fodor E, Schofield CJ, Gileadi O, McHugh PJ. Characterization of the SARS-CoV-2 ExoN (nsp14ExoN-nsp10) complex: implications for its role in viral genome stability and inhibitor identification. Nucleic Acids Res. 2022;50(3):1484-1500. doi: 10.1093/nar/gkab1303
20. Son J, Huang S, Zeng Q, Bricker TL, Case JB, Zhou J, Zang R, Liu Z, Chang X, Darling TL, Xu J, Harastani HH, Chen L, Gomez Castro MF, Zhao Y, Kohio HP, Hou G,

Fan B, Niu B, Guo R, Rothlauf PW, Bailey AL, Wang X, Shi PY, Martinez ED, Brody SL, Whelan SPJ, Diamond MS, Boon ACM, Li B, Ding S. JIB-04 has broad-spectrum antiviral activity and inhibits SARS-CoV-2 replication and coronavirus pathogenesis. mBio. 2022;13(1):e0337721. doi: 10.1128/mbio.03377-21

21. Beacon TH, Delcuve GP, Davie JR. Epigenetic regulation of ACE2, the receptor of the SARS-CoV-2 virus[1]. Genome. 2021;64(4):386-399. doi: 10.1139/gen-2020-0124
22. Knyazev E, Maltseva D, Raygorodskaya M, Shkurnikov M. HIF-dependent NFATC1 activation upregulates ITGA5 and PLAUR in intestinal epithelium in inflammatory bowel disease. Front. Genet. 2021;12:791640. doi: 10.3389/fgene.2021.791640
23. Yamane K, Tateishi K, Klose RJ, Fang J, Fabrizio LA, Erdjument-Bromage H, Taylor-Papadimitriou J, Tempst P, Zhang Y. PLU-1 is an H3K4 demethylase involved in transcriptional repression and breast cancer cell proliferation. Mol. Cell. 2007;25(6):801-812. doi: 10.1016/j.molcel.2007.03.001
24. Rajput K, Ansari MN, Jha SK, Medatwal N, Sharma P, Datta S, Kar A, Pani T, Cholke K, Rana K, Khan A, Mukherjee G, Deo SVS, Prabhu JS, Mukhopadhyay A, Bajaj A, Dasgupta U. RICTOR drives ZFX-mediated ganglioside biosynthesis to promote breast cancer progression. bioRxiv. 2022.01.10.475595. doi: 10.1101/2022.01.10.475595
25. Bamodu OA, Huang WC, Lee WH, Wu A, Wang LS, Hsiao M, Yeh CT, Chao TY. Aberrant KDM5B expression promotes aggressive breast cancer through MALAT1 overexpression and downregulation of hsa-miR-448. BMC Cancer. 2016;16:160. doi: 10.1186/s12885-016-2108-5
26. Dey BK, Stalker L, Schnerch A, Bhatia M, Taylor-Papidimitriou J, Wynder C. The histone demethylase KDM5b/JARID1b plays a role in cell fate decisions by blocking terminal differentiation. Mol. Cell. Biol. 2008;28(17):5312-5327. doi: 10.1128/MCB.00128-08
27. Dabiri Y, Gama-Brambila RA, Taškova K, Herold K, Reuter S, Adjaye J, Utikal J, Mrowka R, Wang J, Andrade-Navarro MA, Cheng X. Imidazopyridines as potent KDM5 demethylase inhibitors promoting reprogramming efficiency of human iPSCs. iScience. 2019;12:168-181. doi: 10.1016/j.isci.2019.01.012
28. Kuo KT, Huang WC, Bamodu OA, Lee WH, Wang CH, Hsiao M, Wang LS, Yeh CT. Histone demethylase JARID1B/KDM5B promotes aggressiveness of non-small cell lung cancer and serves as a good prognostic predictor. Clin. Epigenetics. 2018;10(1):107. doi: 10.1186/s13148-018-0533-9
29. Schonfeld M, Averilla J, Gunewardena S, Weinman SA, Tikhanovich I. Male-specific activation of lysine demethylases 5B and 5C mediates alcohol-induced liver injury and hepatocyte dedifferentiation. Hepatol. Commun. 2022;6(6):1373-1391. doi: 10.1002/hep4.1895
30. Nikulin SV, Mnafki (Krainova) NA, Shilin SA, Gazizov IN, Maltseva DV. Ribosome inactivation and the integrity of the intestinal epithelial barrier. Mol. Biol. (Mosk). 2018;52(4):675-682. doi: 10.1134/S0026898418040146